Article citation info:
Sawczuk W, Kaczmarek D, Jüngst M. Model of energy consumption by brake discs of rail vehicles. Rail Vehicles/Pojazdy Szynowe. 2024;1-2:11-20. https://doi.org/10.53502/RAIL-186984

Rail Vehicles/Pojazdy Szynowe

www.railvehicles.eu

Model of energy consumption by brake discs of rail vehicles

Wojciech **Sawczuk** [a], Daniel **Kaczmarek** [b], Mateusz **Jüngst** [a]

[a] *Faculty of Civil and Transport Engineering, Poznan University of Technology, Poznan, Poland*
[b] *ATC Group Sp. z o. o, Gostyn, Poland*

ARTICLE INFO

Received: 20 February 2024
Revised: 12 March 2024
Accepted: 9 April 2024
Available online: 15 April 2024

KEYWORDS

Brake disc
Ventilation
Energy consumption
Losses on the disc fan

The aim of the article is to present a computational model to determine the losses generated by the brake discs of rail vehicles. The energy consumption of the disc (energy losses) is divided into inertia losses and fan losses. The article is preceded by a review of the design solutions of brake discs of rail vehicles in terms of their ventilation and cooling after braking. Particular attention was paid to three types of brake disc designs with ventilation blades, bars and other shapes of ventilation bridges, and how the ventilation of these discs affects energy losses. On the one hand, forced ventilation of brake discs shortens the cooling time after intensive braking, on the other hand, it causes energy losses due to forced ventilation when the brakes are not used. The article presents the state of knowledge regarding the cooling efficiency of brake discs as a result of forced ventilation and presents a method for calculating the energy consumption generated by the brake disc in relation to the rotational speed. The energy losses were divided in the article into inertia losses due to the rotating mass and losses on the fan, in which the energy necessary for the rotation of the brake disc was determined from the method of calculating centrifugal fans with known geometric dimensions.

1. Introduction

From 2020, the European Green Deal strategy related to the transition to clean energy was introduced in the European Union countries. Broadly speaking, this is to reduce greenhouse gas emissions and improve our quality of life. The European Commission has adopted a package of legislative proposals to adapt the EU's climate, energy, tax and transport policies to meet the goal of reducing greenhouse gas emissions by at least 55% by 2030. compared to the level in 1990 [15]. The assumptions of the Green Deal also require lower emissions of harmful substances as well as lower energy consumption on means of transport [6]. In terms of emissions of harmful substances, including CO_2 [27], work is being carried out on new hydrogen-powered combustion engines [21], at the TRAKO fair in Gdansk in 2023, among others. the first diesel shunting locomotive powered by hydrogen was presented [7, 8]. Other manufacturers offer vehicles with hybrid drives [4, 18, 26] or electric drives [22, 35] for reduced emissions.

In terms of reducing the consumption of fuel or electricity [5] in rail vehicles, steels with increased strength properties [2, 19] and carbon fiber composite materials described in the works [20] are introduced in the drive structure [10] and vehicle construction. At the InnoTrans international railway technology fair in Berlin in 2014, a Kawasaki bogie for a passenger vehicle with a rocker beam made of carbon fiber was presented for the first time, which reduced the weight of the bogie by approximately 40% compared to the traditional steel structure [23].

In the field of friction braking systems, work has been carried out for several years to reduce the emissions of solid wear products from friction linings, described, among others, in the works [1, 11], as well as the complete elimination of copper as a component of friction linings [14, 17] in favor of organic components. Work has been carried out for several years on modeling the consumption of solid friction products

* Corresponding author: wojciech.sawczuk@put.poznan.pl (W. Sawczuk)

described in [24], and the entry into force of the new EURO 7 standard will force work to be carried out in the field of gas emissions from the braking system [36]. It is possible to recover part of the energy from the braking process by eliminating friction braking [31]. Currently, this occurs in the case of electric or diesel locomotives with electric transmission as well as with diesel or electric multiple units (EMU), including metro vehicles and trams (light rail vehicles) [34].

In all the above-mentioned vehicles, the drive system at the wheelset consists of an electric motor, which operates in generator mode during braking, generating additional resistance that reduces the vehicle's speed. It is called electrodynamic braking ED. The resulting current in the windings of the traction motor operating as a generator can be fed back to the traction network. A vehicle located in its close vicinity when the starter is on can absorb driving energy recovered from braking the vehicle in front of it. This process is called recuperation, and in practice it is only possible in the case of public transport vehicles such as trams [3, 16]. In railway vehicles, energy is transferred to the traction network, lost as heat or released in braking resistors (Fig. 1a, b). In newer vehicles, energy is recovered and stored in the so-called energy storage tanks super capacitors (Fig. 1c). This solution allows you to reduce energy consumption by approximately 30% [38].

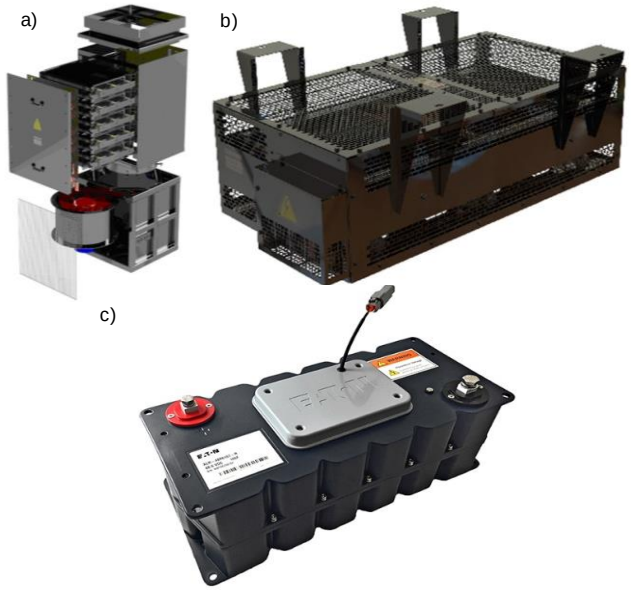

Fig. 1. View of: a) braking resistors mounted inside the vehicle, b) braking resistors mounted on the roof from Simpax, c) super capacitor from Eaton [9, 30]

In the case of electric multiple units, during intensive braking, it is possible to implement electrodynamic braking with a blending function on the drive bogies (so-called brake blending) [12]. The majority of the braking force is provided by the electrodynamic brake; in the first phase of braking, depending on the set braking force on the travel and braking controller, the friction brake (electro-pneumatic EP) is used to a small extent, as shown in Fig. 2. In the second phase of braking, the force of the electrodynamic brake is sufficient. to implement braking (sometimes its operation should be limited, the so-called cutting off the ED brake characteristic). The third braking phase at a speed of approximately 10 km/h causes the effectiveness of the ED brake to drop to zero and the friction brake to be activated [37].

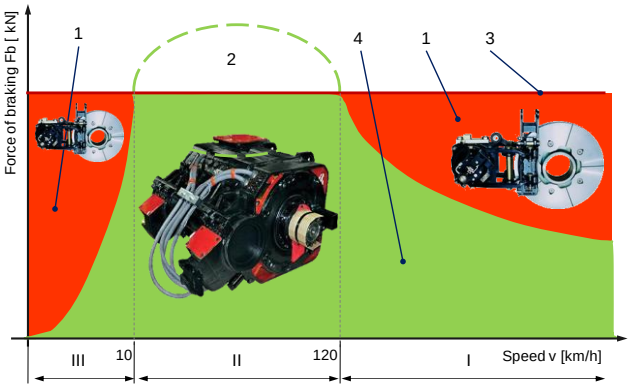

Fig. 2. Example characteristics of an electrodynamic brake performing blending: 1 – missing the braking force, 2 – reducing the force of the electrodynamic brake, 3 – the desired (required) braking force, 4 – full operation of the electrodynamic brake, I – first phase of ED+EP braking, II – second phase of ED braking, III – third phase of braking, advantage of the EP brake

The aim of the article is to present a method for determining energy losses generated by a railway ventilated brake disc. The energy consumed by the discs when the brake is off has been divided into two parts. The first is the inertial energy resulting from the rotation of the disc, which is a rigid body, and the energy lost on ventilation and the phenomenon of air pumping due to forced ventilation.

2. Overview of the design of ventilated brake discs

In railway technology, three types of ventilation are used in the field of ventilated discs. The first method of cooling brake discs were ventilation blades radially distributed between the inner surfaces of the friction rings. Figure 3 shows a view of the wheelset with two and three ventilated brake discs mounted on the wheelset axis. The number of brake discs on the axle depends on the speed at which the rail vehicle will be operated. For passenger wagons designed for a speed of 200 km/h, two discs are used on the axle, and at higher speeds of approximately 250–300 km/h, three brake discs are used to stop the vehicle within the required braking distance. Three brake discs ac-

cording to [25] increase the mass of the wheelset. Railway technology also uses four brake discs mounted on the axle of the wheel set in high-speed vehicles. However, these are not ventilated discs, but full discs made of alloy steel [32].

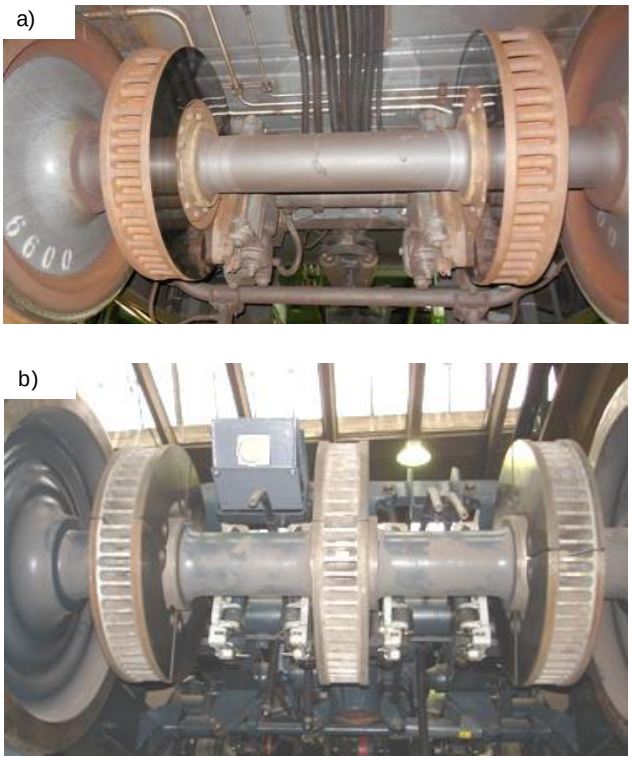

Fig. 3. View of the wheelset: a) with two ventilated discs on the axis, b) with three ventilated discs on the axis of the wheelset

The second type of ventilated discs are discs with ventilating round bars, and the third type is oval bars. Figure 4, using the example of mounted wheel discs of a wheel set, shows a comparative view of a disc with ventilating blades and round bars.

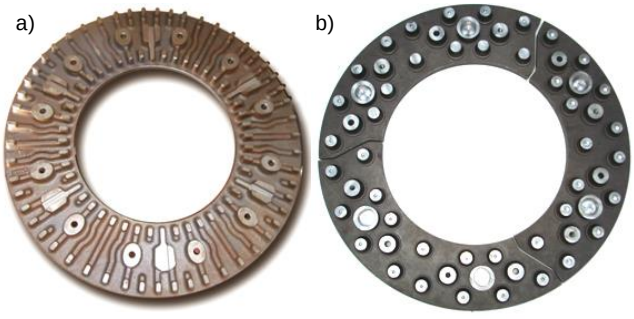

Fig. 4. View of a brake disc mounted to the wheel of a wheelset with: a) ventilation blades [45], b) ventilation round bars [29]

In terms of implementation, brake discs with ventilating blades are simpler to make than discs with ventilating rods. Both discs are made of gray iron or cast steel castings, and the difficulty and time-consuming results from preparing the sand mold and making models of ventilation ducts. In the case of a disc with ventilating blades, the cores replacing the cooling blades are made in the form of wedge-shaped flat bars, which are then inserted circumferentially from the outer radius into the interior of the mold. In the case of discs with ventilating bars or bridges, the mold making process is more complex and time-consuming.

In addition to the method of ventilation of the brake disc, material issues are also of great importance, affecting the effectiveness and speed of cooling of the disc. Also taking into account that half of the wagon's weight is the running gear and brakes, in 1992 the Knorr-Bremse company began research using light metals for brake discs. The best results were obtained when an aluminum alloy containing 20% of pure ceramic powder was used for the brake disc (Fig. 5) [42].

Fig. 5. View of a brake disc made of an aluminum-ceramic alloy by Knorr-Bremse

The main advantages of light alloy brake discs include a 25% better ability to dissipate heat compared to cast iron discs. Tests have shown that due to good cooling, two aluminum discs have the same effectiveness as three cast iron discs [39].

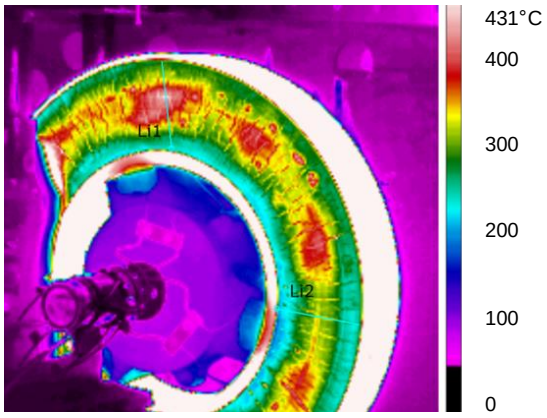

Fig. 6. Image from a thermal imaging camera of the brake disc after stopping braking with visible hot-spots [25]

It should be emphasized that the main operational problems of ventilated brake discs are microcracks

resulting from cyclic heating and cooling, as well as hot-spots occurring after frequent braking at high speeds [40]. Figure 6 shows a thermal image of the brake disc after braking from a speed of 200 km/h with visible hot-spots and cracks that were only visible using an IR camera. When analyzing the designs of brake discs used in rail vehicles, it should be emphasized that they result primarily from issues related to the braking ability of the vehicle (stopping on a given braking distance), their effective cooling and the technology of their production. The next chapter presents the impact of shield design on energy losses.

3. Influence of brake discs design on ventilation process

The studies presented in [28, 41] have shown that discs ventilated with blades or rods (or with other shapes) increase the energy consumption for cooling them through continuous rotation. Discs with blades generate the highest energy consumption compared to other solutions, as shown in Fig. 7.

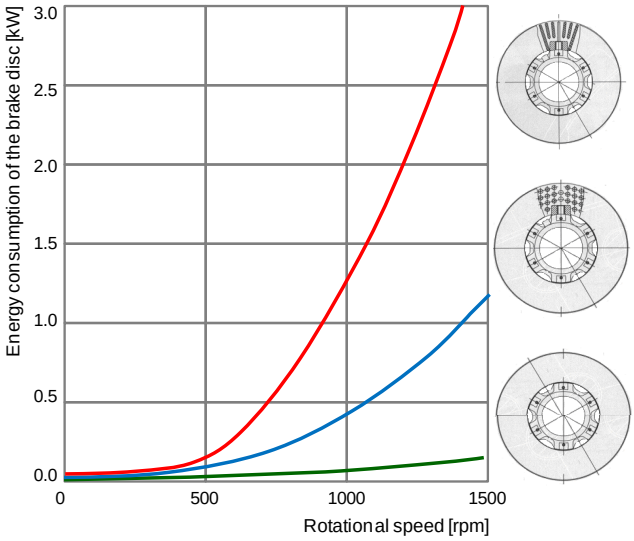

Fig. 7. Energy consumption of railway brake discs [26]

Analyzing the graph presented in Fig. 7, it is concluded that the ventilation bars generate approximately 60% lower energy consumption compared to the disc with blades. Moreover, research conducted by [26] proved that a disc with cooling rods or other thermal bridges achieves greater braking power by approximately 3% compared to a disc with blades. It should be noted that, according to work [33], forced ventilation inside the disc does not affect the lower values of temperature obtained during braking by the disc. Both ventilated and non-ventilated discs will obtain the same or similar temperature values under the same braking conditions. Only a ventilated disc will cool down to the ambient temperature faster after braking and driving at a constant speed than a solid, unventilated disc. Figure 8 shows the dependence of the temperature of discs of the same diameter (640 mm) on the cooling time during simulated driving at a constant rotational speed of 1000 rpm.

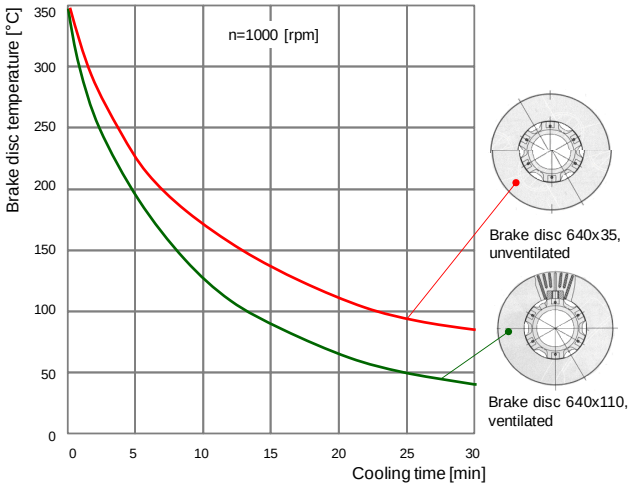

Fig. 8. Dependence of temperature on cooling time of brake discs (ventilated and unventilated) [28]

In the field of automotive and railway brake discs, work has been carried out for many years on modifying the air flow through the disc with additional holes in the friction rings. Drilling in the friction surface allows for additional heat exchange. As indicated in [44], the static pressure prevailing on the outer surfaces of the disc is usually higher than inside the ventilation channels, which allows additional air masses to be sucked into the center of the disc through these holes (Fig. 9).

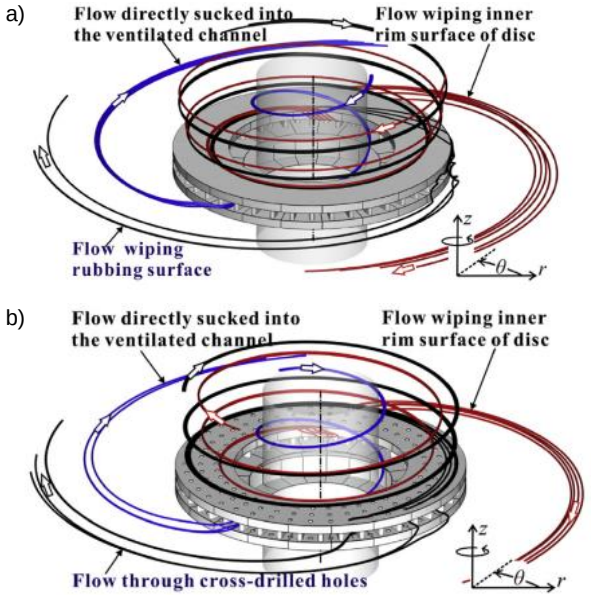

Fig. 9. 3D flowlines summarizing the overall flow patterns for a) standard and b) drilled brake disc [44]

The internal flow in a disc with standard blades, due to the expansion of the ventilation channel towards the outer edge of the disc, leads to the creation of an unfavorable pressure gradient in the radial direction, which results in flow recirculation. The introduction of holes allows for a significant reduction in this phenomenon by directing the streams from the holes to areas where areas of lower static pressure appeared in the standard disc (Fig. 10) [43].

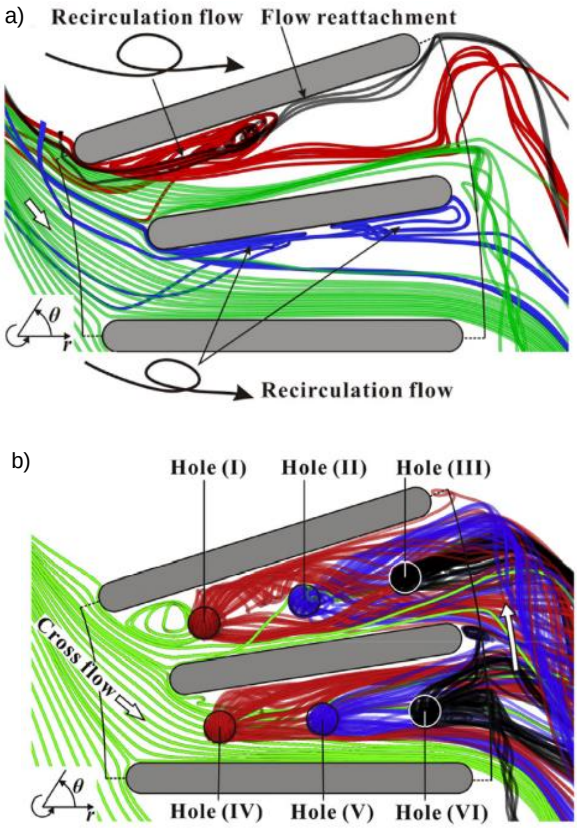

Fig. 10. Comparison of internal flow: a) for standard disc, b) for drilled disc [43]

The introduction of holes leads to a reduction in the heat capacity of the disc friction rings. As a result, with lower loads and shorter braking times, the drilled disc reaches slightly higher temperatures. However, during long-term braking at higher speeds, the drilled disc shows its superiority by presenting a much lower surface temperature.

An interesting solution was presented in [44]. Its authors developed a completely new shield structure, where the previously used structure of ventilation channels with blades was replaced with a special X-mesh structure (Fig. 11). Its introduction allowed for very uniform heat exchange and thus uniform temperature distribution. Generally speaking, a disc with an X-mesh gives an average Nusselt number Nu that is 18–21% higher than a disc with ventilation blades. It was pointed out that the new structure, however, leads to a reduction in the pumping efficiency of the disc, which, while it may indeed be a problem in automotive applications, may provide tangible benefits in railway applications.

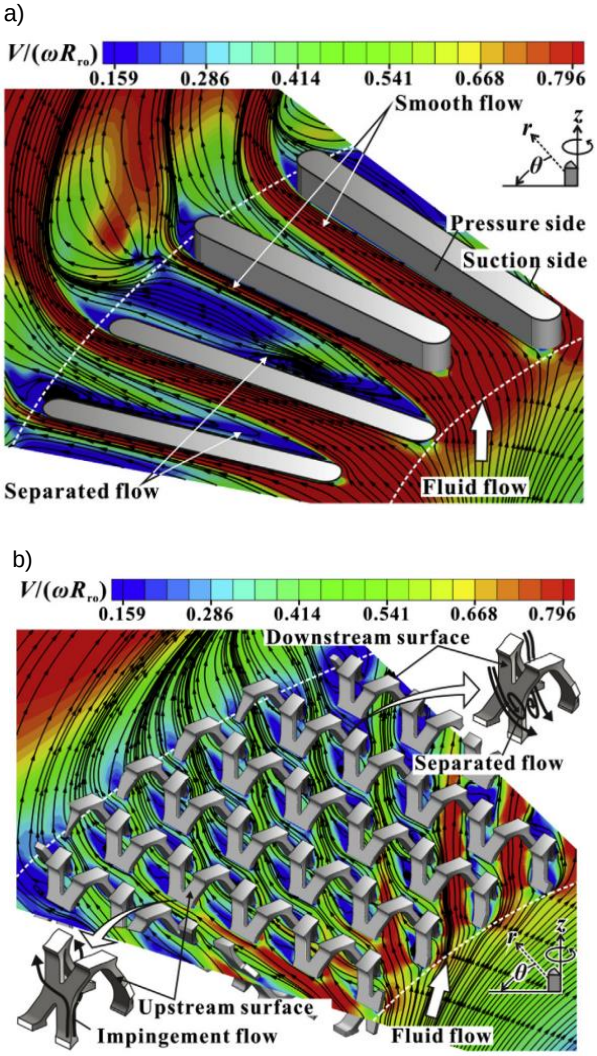

Fig. 11. Comparison of internal flows shown by flow lines and velocity distribution: a) disc with blades [44]. b) improved shield with X grid [44]

From the point of view of railway applications, a very important publication in the field of FEM numerical analyzes is the study [44], focused on issues related to air flow in the ventilation channels of the shield and the related convective heat transfer. The author undertook to develop a new shield that was a synthesis of the design solutions of other railway shields: he used a row of tangential blades and then shorter radial blades closer to the center of the shield. A few years after the design and experimental tests, the three-dimensional model of the shield was subjected to CFD analyses. The simulation assumed rotation of the disc in a medium in a steady state (without air movement) at a speed of 1500 rpm. Figure 12a shows a diagram of the flow through the middle sec-

tion of the disc for a speed of 500 rpm. The shape of the blades and the rotational direction of airflow through the disc are clearly visible. A high flow velocity (11 m/s) can be observed between the blade and the front face (area a) and stagnation and turbulence (area b) on the rear face. It should be remembered that railway discs must have the same characteristics regardless of the direction of rotation – they cannot be directional [36].

Figure 12b shows the distribution of the local convective heat transfer coefficient on the blades and connectors for a disc heated to 200°C at a speed of 1500 rpm in steady air at a temperature of 20°C. The results clearly indicated large local variations of the coefficient. The lowest values of approximately 7 W/m^2 K (corresponding to natural convection) were recorded in places of turbulence – area b. The highest values of 118 W/m^2 K were recorded in areas with the maximum flow velocity – in area a. The importance of the total average heat transfer coefficient must be emphasized because this value, multiplied by the total flowing area of the disc, determines the total convective power output (heat dissipation rate) used in the design calculations [36].

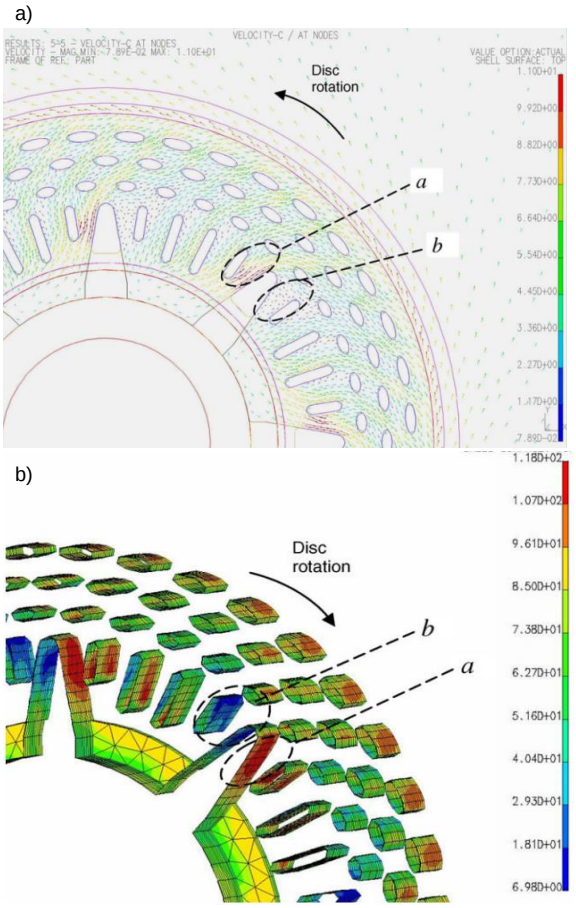

Fig. 12. a) flow velocity diagram for the new disc at a speed of 500 rpm, b) distribution of the convective heat transfer coefficient in the disc channels [37]

The article [37] indicates a very interesting aspect of optimizing the design of brake discs: achieving a balance between cooling efficiency and power losses resulting from pumping.

4. Model of energy consumption by a railway disc brake

The energy consumption generated by the brake disc should be divided into two parts, i.e. due to the rotating mass (inertia losses) and due to ventilation, in accordance with the relationship (1).

$$N_T = N_I + N_V \text{ [kW]} \tag{1}$$

where: N_T – total energy consumption, N_I – energy consumption on the inertia of the brake disc, N_v – energy consumption due to ventilation.

A similar division of energy consumption by a brake disc was presented in [26], but the calculation method was presented on brake discs that were smaller in diameter. In order to determine the energy consumed by the disc per rotation, it is necessary to use the following data, presented in Table 1, calculations were carried out for a 640×110 disc. In rail vehicles, such as passenger or freight wagons, three types of discs are used with dimensions (outer diameter × width), 590×110, 610×110 and 640×110. These are the most commonly used dimensions, but there are disc designs with widths of 80, 150 and 180 mm.

Table 1. Input quantities for calculating the energy consumption of a brake disc as a rigid body in rotation

No.	Input quantities	Symbol, value, unit
1	The mass of the disc with ventilation blades	m_b = 149.08 kg
2	Weight of the disc with ventilation bars	m_r = 136.65 kg
3	Outer diameter of the disc	D = 640 mm
4	Inner diameter of the disc	d = 350 mm
5	Density of cast iron	ρ_z = 7200 kg/m^3
6	Acceleration at start-up	a = 1.0 m/s^2
7	Disc rotation speed	n = 1000 rpm

Due to the complex shape, first of all, the volume of the discs (e.g. with ventilation blades) should be determined using the formula (2).

$$V = \frac{m_b}{\rho_z} = \frac{149.08}{7200} = 0.0207 \text{ m}^3 \tag{2}$$

With the volume of the disc known, the thickness of the disc is then calculated from equation (3).

$$g_z = \frac{V}{\left(\frac{\pi D^2}{4} - \frac{\pi d^2}{4}\right)} = \frac{0.0207}{\left(\frac{3.14 \cdot 0.64^2}{4} - \frac{3.14 \cdot 0.35^2}{4}\right)} = 0.0918 \text{ m} \tag{3}$$

The moment of inertia of the disc was calculated from formula (4).

$$I = \frac{1}{2}m\left(\frac{D^2}{4} + \frac{d^2}{4}\right) = \frac{1}{2}149.08\left(\frac{0.64^2}{4} + \frac{0.35^2}{4}\right) = \\ = 9.91\ \text{kg} \cdot \text{m}^2 \quad (4)$$

The angular speed of the brake disc at a rotational speed of 1000 rpm was determined from the equation (5):

$$\omega = \frac{d\varphi}{dt} = \frac{2\pi n}{60} = \frac{2 \cdot 3.14 \cdot .1000}{60} = 104.7\ \frac{\text{rad}}{\text{s}} \quad (5)$$

The angular acceleration of the brake disc during start-up was determined from equation (6):

$$\varepsilon = \frac{d\omega}{dt} = \frac{a}{\frac{D}{2}} = \frac{1}{\frac{0.64}{2}} = 3.13\ \frac{\text{rad}}{\text{s}^2} \quad (6)$$

The startup time for the brake disc up to a rotational speed of 1000 rpm was determined from the formula (7):

$$t = \frac{\omega}{\varepsilon} = \frac{104.7}{3.13} = 33.51\ \text{s} \quad (7)$$

The kinetic energy in the rotation of the brake disc was determined from equation (8):

$$E_k = \frac{I \cdot \omega^2}{2} = \frac{9.91 \cdot 104.7^2}{2} = 54.37\ \text{kJ} \quad (8)$$

The energy consumption of the brake disc for speed n was determined from the following relationship (9):

$$N_d = \frac{dE}{dt} = \frac{E_k}{1000t} = 1.62\ \text{kW} \quad (9)$$

This is a calculation of the energy necessary to rotate the brake disc at one rotational speed. For the disc with ventilating rods, the inertial resistance is N_r = = 1.49 kW and is approximately 9% lower than the disc with ventilating blades.

Determining the energy consumption of a brake disc fan is more complex than the inertia losses. In this case, the brake disc is considered as a centrifugal radial fan and the methodology given in [13, 39] is followed. First, it is necessary to know the parameters listed in Table 2.

Table 2. Input quantities for calculating the energy consumption of the brake disc fan in rotation

No.	Input quantities	Symbol, value, unit
1	Internal diameter of the blade ring	d = 350 mm
2	Outer diameter	D = 640 mm
3	Width of the rim at the inlet	b_1 = 70 mm
4	Width of the rim at the outlet	b_2 = 70 mm
5	Blade entry angle	β_1^* = 90°
6	Blade outlet angle	β_2^* = 90°
7	Number of blades	Z = 60
8	Blade length	L = 140 mm
9	Rotation speed	n = 1000 rpm
10	Air density	ρ = 1.2 kg/m^3
11	Inlet pressure	p_1 = 100 kN/m^2

According to the methodology given in [13, 38], fan calculations are reduced to angular and peripheral speeds, blade ring filling, conventional Reynolds number, wading power, absolute velocity at the blade outlet, rated efficiency, rotor aspect ratio (read from the tables), the stream deflection angle, the increase in peripheral speed and the work provided to the medium (theoretical accumulation). Then, the compression work is calculated from the energy balance by first determining the compressibility coefficient. This is a calculation of one operating point of the radial rotor. To find further characteristic points, proceed in the same way, substituting subsequent values of the brake disc rotational speed. Using this methodology for a centrifugal fan, the characteristics of the fan's driving power, static concentration and air flow efficiency through the impeller are determined as a function of efficiency and rotational speed.

Analyzing the characteristics of radial brake disc fans, it is found that the energy consumption of the disc fan increases progressively with the increase in rotational speed. This is because the energy consumption by the brake disc is described by a power function in accordance with the proposed relationship (10):

$$N_V = w \cdot n^3\ [\text{kW}] \quad (10)$$

where: w – disc fan form factor, n – disc rotation speed [rpm].

Apart from the strong effect of the disc speed, the course of energy losses due to forced ventilation is also influenced by the shape factor of the disc fan, which is described as a function of the following quantities:

$$w = f(D, d, b_1, b_2, \beta_1^*, \beta_2^*, Z, l, \rho) \quad (11)$$

On this basis, the authors of the article concluded that it is possible to simplify the methodology for determining the energy losses of a brake disc by introducing several simplifications such as $b_1 = b_2 = b$, $\beta_1^* = \beta_2^* = 90°$ and constant air density at the inlet and outlet of the blade ρ = 1.2 kg/m^3.

Ultimately, the form factor of the disc fan after taking into account the above simplifications is a function of the following quantities:

$$w = f(D, d, b, Z, l) \quad (12)$$

After substituting all the equations from the centrifugal fan calculation methodology and applying the proposed simplifications, the relationship (13) was determined to calculate the energy consumption of the brake disc fan.

$$N_V = 6.66 \cdot 10^{-3} n^2 d^2 Db \cdot \\ \cdot \left[0.048nD + 0.03\frac{d^2}{D}\text{ctg}\left\{90^o - \frac{3b\left(90^o - \text{arctg}\frac{0.65d^2}{D}\right)}{D - d\sqrt{\frac{0.637Zl}{d+D}}} + 2^o\right\}\right] \quad (13)$$

By comparing both methods: the computational method from references [13, 39] and the simplified one from equation (13), the waveforms of power losses on the fan are obtained with an average difference in results of 2.2%. This is due to the fact that the conventional Reynolds number increases with the increase in the rotational speed of the brake disc. On its basis, the coefficient *k* is read from the graph [13], depending on Re, and its value decreases as the Reynolds number increases. When deriving the final relationship (13) for the power consumed by the disc fan, the *k* factor was averaged.

5. Calculation results

Figure 13 shows the characteristics of energy consumption of a brake disc being a rigid body in rotation (old inertia) without ventilation as a function of rotational speed.

Due to its slightly lower weight, a brake disc with ventilating bars has slightly lower energy consumption than a paddle disc. For comparison, the graph shows inertia losses for a 640×35 solid disc of the same diameter made of alloy steel.

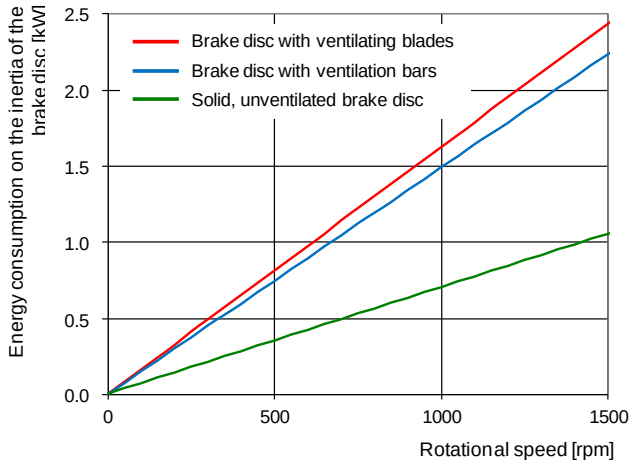

Fig. 13. Inertia losses of brake discs in rotation (without ventilation)

The sum of the inertial resistance and the resistance posed (generated) by the brake disc fan in rotation is shown in Fig. 14. Analyzing the energy consumption characteristics of the brake disc in rotation based on the graphs presented in Fig. 13, it is concluded that up to a speed of approximately 500 rpm there are only inertial resistances of the brake disc.

Work on energy consumption by ventilated brake discs proves that in order to precisely understand the phenomena that accompany the process of pumping air through the discs, it is also necessary to model the air flow on the chassis of a rail vehicle. Further directions of the authors' work will be carried out in this area.

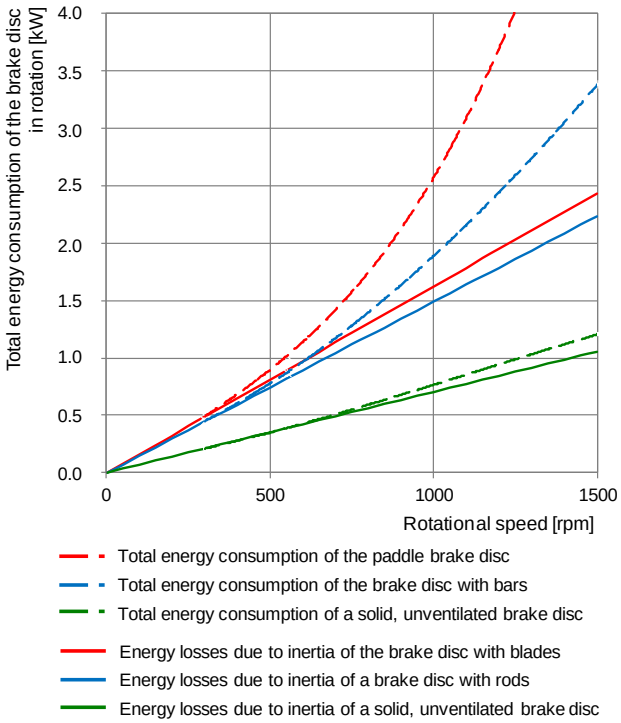

Fig. 14. Total energy consumption of the brake disc in rotation (inertia and disc ventilation)

6. Conclusions

Simulations regarding the air flow around and inside the brake discs are carried out in terms of the efficiency of heat exchange of the disc with the surroundings. Mainly, scientific works focus on the phenomenon of disc pumping due to fan operation without taking into account the air momentum resulting from the linear direction of vehicle movement. These works and simulation tests are also carried out to determine the energy losses generated by brake discs. As a consequence, this increases the fuel consumption of motor vehicles. In the case of railway vehicles – to higher electricity consumption.

The computational model presented in the article makes it possible to estimate the energy consumption due to the inertia of the disc in rotation and due to the ventilation process itself. This makes it possible to divide the total energy consumption of the disc due to the inertia and ventilation of the disc when pumping air into the cooling process.

Analyzing the calculation chart, it is found that despite the same size of the 640×110 discs, the rod disc causes over 9% lower inertial resistance than the paddle disc in the entire rotational speed range.

The greatest share of inertial resistance due to the disc mass in rotation occurs at speeds up to 500 rpm

for ventilated discs and up to approximately 750 rpm for solid (non-ventilated) discs. A further increase in rotational speed increases energy consumption due to ventilation and air pumping.

The presented algorithm for determining the power of a brake disc fan makes it possible to determine the energy consumption due to forced ventilation without conducting expensive bench tests. The maximum error made during calculations does not exceed 2.2%.

Using the methodology for calculating the energy consumption of the brake disc (relationships (1)–(9)) due to the disc inertia and the methodology for energy losses on the fan (relationship (13)), it is possible to determine energy losses not only for the standardized disc brakes of passenger cars presented in UIC 541-3 card, but also for other shield designs that are not covered by the above card. This applies in particular to single discs mounted on both sides of the wheels of locomotives, rail cars, rail buses and public transport vehicles. The only condition that must be met to calculate losses on the fan is knowledge of the geometric dimensions of the brake disc.

Acknowledgements 11

The investigations were carried out within the Research Subsidy SBAD 0416/SBAD/0006 in the year 2024.

Nomenclature

CFD	computational fluid dynamics
ED	electrodynamic brake
EMU	electric multiple unit
EP	electropneumatic brake
IR	infrared
MES	finite element method
Nu	Nusselt number
Re	Reynolds
UE	European Union

Bibliography

[1] Anoop S, Natarajan S, Kumaresh Babu SP. Analysis of factors influencing dry sliding wear behavior of Al/SiCp–brake pad tribosystem. Materials and Design. 2009;30:3831-3838. https://doi.org/10.1016/j.matdes.2009.03.034

[2] Bajerlein M, Czerwiński J, Merkisz J, Daszkiewicz P, Rymaniak Ł. Wysokotemperaturowa stal stopowa wykorzystywana w pojazdach kolejowych (in Polish). TTS Technika Transportu Szynowego. 2017;24(12):228-232.

[3] Bartłomiejczyk M. Rekuperacja energii hamowania w praskim systemie tramwajowym (in Polish). TTS Technika Transportu Szynowego. 2015;1-2:50-53.

[4] Bieniek A, Graba M, Mamala J, Prażnowski K, Hennek K. Energy consumption of a passenger car with a hybrid powertrain in real traffic conditions. Combustion Engines. 2022;191(4):15-22. https://doi.org/10.19206/CE-142555

[5] Cieślik W, Szwajca F, Golimowski J. The possibility of energy consumption reduction using the ECO driving mode based on the RDC test. Combustion Engines. 2020;182(3):59-69. https://doi.org/10.19206/CE-2020-310

[6] Daszkiewicz P, Kołodziejek D. Comparison and analysis of modern combustion powertrain systems of rail vehicles. Combustion Engines. 2024;196(1):46-53. https://doi.org/10.19206/CE-171385

[7] Durzyński Z. Hydrogen-powered drives of the rail vehicles (part 1). Rail Vehicles/Pojazdy Szynowe. 2021;2:29-40. https://doi.org/10.53502/RAIL-139980

[8] Durzyński Z. Hydrogen-powered drives of the rail vehicles (part 2). Rail Vehicles/Pojazdy Szynowe. 2021;3:1-11. https://doi.org/10.53502/RAIL-142694

[9] EATON Powering Business Worldwide: https://www.eaton.com/us/en-us/catalog/electronic-components/xlr-supercapacitor-module.html (accessed on 14.02.2024)

[10] Elzayady N, Elsoeudy R. Microstructure and wear mechanisms investigation on the brake pad. J Mater Process Tech. 2021;11:2314-2335. https://doi.org/10.1016/j.jmrt.2021.02.045

[11] Energy and the Green Deal, Clean Energy Transition: https://commission.europa.eu/strategy-and-policy/priorities-2019-2024/european-green-deal/energy-and-green-deal_pl (accessed on 14.02.2024)

[12] Far M, Gallas D, Urbański P, Woch A, Mieżowiec K. Modern combustion-electric PowerPack drive system design solutions for a hybrid two-unit rail vehicle. Combustion Engines. 2022;190(3):80-87. https://doi.org/10.19206/CE-144724

[13] Idris UD, Aigbodion VS, Akubakar IJ, Nwoye CI. Eco-friendly asbestos free brake-pad: using banana peels. Journal of King Saud University – Engineering Sciences. 2015;27:185-192. https://doi.org/10.1016/j.jksues.2013.06.006

[14] Park J, Joo B, Seo H, Song W, Lee JJ, Lee WK, Jang H. Analysis of wear induced particle emissions from brake pads during the worldwide harmonized light vehicles test procedure (WLTP). Wear. 2021;466-467:203539. https://doi.org/10.1016/j.wear.2020.203539

[15] Kuczewski S. Wentylatory. Wydawnictwo Naukowo-Techniczne. Warsaw 1978.

[16] Maciołek T, Drążek Z. Zasobnik energii w tramwaju zmniejszający zużycie energii (in Polish). TTS Technika Transportu Szynowego. 2004;10:54-57.

[17] Mahale V, Bijwe J. Exploration of plasma treated stainless steel swarf to reduce the wear of copper-free brake-pads. Tribol Int. 2020;144:106111. https://doi.org/10.1016/j.triboint.2019.106111

[18] Mamala J, Śmieja M, Prażnowski K. Analysis of the total unit energy consumption of a car with a hybrid drive system in real operating conditions. Energies. 2021;14(13):3966. https://doi.org/10.3390/en14133966

[19] Matej J, Orliński P. Reducing wheel wear of a motorised metro car on a curved track with a small curve radius. Rail Vehicles/Pojazdy Szynowe. 2023;3-4:25-32. https://doi.org/10.53502/RAIL-175921

[20] Nishimura T. efWING–New-Generation Railway Bogie. Japanese Railway Engineering. 2016;194:13-14.

[21] Nishimura T, Taga Y, Ono T, Konoike F, Tsumura Y, Inamura F et al. efWING–New-Generation Railway Bogie. Kawasaki Technical Review. 2016;177:27-32.
[22] Pielecha I, Cieślik W, Borowski P, Czajka J, Bueschke W. The development of combustion engines for hybrid drive systems. Combustion Engines. 2014;158(3):23-35. https://doi.org/10.19206/CE-116934
[23] Pielecha I, Engelmann D, Czerwiński J, Merkisz J. Use of hydrogen fuel in drive systems of rail vehicles. Rail Vehicles/Pojazdy Szynowe. 2022;1-2:10-19. https://doi.org/10.53502/RAIL-147725
[24] Regulski P. Assessment of the life cycle of city buses with diesel and electric drive in the operation phase. Combustion Engines. 2023;193(2):117-121. https://doi.org/10.19206/CE-162108
[25] Sawczuk W, Rilo Cañás AM. The issues of hot-spots type in the railway disc brake. Rail Vehicles/Pojazdy Szynowe. 2021;1:33-43. https://doi.org/10.53502/RAIL-138492
[26] Sawczuk W, Rilo Cañás AM, Kołodziejski S. Evaluation of weight wear of disc brake pads after test stands. Rail Vehicles/Pojazdy Szynowe. 2022;3-4:53-59. https://doi.org/10.53502/RAIL-162350
[27] Sawczuk W, Jüngst M. Tarcze hamulcowe pojazdów szynowych (in Polish). TTS Technika Transportu Szynowego. 2016;12:496-502.
[28] Sawczuk W. Selected issues of operational use of rail disc brake. The Archives of Automotive Engineering. 2011; 53(3):41-52. https://doi.org/10.5604/1234754X.1066726
[29] SIEMENS G. Auslegung und Leistungsgrenzen von Scheibenbremsen. ZEV-Glas. Ann. 1988;112(4):139-143.
[30] SIMPAX, We produce resistors: https://www.simpax.pl/pl/rodzaje-rezystorow/rezystory-hamowania/do-pojazdow-trakcyjnych (accessed on 14.02.2024)
[31] Skuza A, Szumska E, Jurecki R. Fuel consumption and CO_2 emission analysis of hybrid and conventional vehicles in urban driving conditions. Combustion Engines. 2023;195(4): 48-55. https://doi.org/10.19206/CE-169569
[32] Słowiński M. An Analysis of CFRP application in the construction of rail vehicles. Problemy Kolejnictwa. 2021;193: 105-103. https://doi.org/10.36137/1935E
[33] Sorochtej M. Kształtowanie jakości zespołu ciernego hamulca tarczowego. Przegląd Kolejowy. 1991;1:15-21.
[34] Szumska E, Jurecki R. Technological developments in vehicles with electric drive. Combustion Engines. 2023; 194(3):38-47. https://doi.org/10.19206/CE-168219
[35] Śmietana K. Euro 7, czyli wątpliwości wokół norm emisji zanieczyszczeń (in Polish). DGP Dziennik Gazeta Prawna. 2023;2(3). https://serwisy.gazetaprawna.pl/ekologia/artykuly/8670843, euro-7-norma-zanieczyszczen-watpliwosci.html
[36] Tirović M. Energy thrift and improved performance achieved through novel railway brake discs. Appl Energ. 2009;86:317-324. https://doi.org/10.1016/j.apenergy.2008.04.017
[37] Urbaniak M, Kardas-Cinal E. Optimization of using recuperative braking energy on a double-track railway line. Transp Res Proc. 2019;40:1208-1215. https://doi.org/10.1016/j.trpro.2019.07.168
[38] Walczak J. Promieniowe sprężarki dmuchawy i wentylatory. Wydawnictwo Politechniki Poznańskiej. Poznan 2013.
[39] Wirth X. Improving the performance of disc brakes on high-speed rail vehicles with a novel types of brake pad: isobar. RTR. 1998;1:24-29.
[40] Wirth X. Disc brakes to stop the world's fastest trains. Railway Gazette February. 1986.
[41] Wu SC, Zhang SQ, Xu ZW. Thermal crack growth-based fatigue life prediction due to braking for a high-speed railway brake disc. Int J Fatigue. 2016;87:359-369. https://doi.org/10.1016/j.ijfatigue.2016.02.024
[42] Varazhun I, Shimanovsky A, Zavarotny A. determination of longitudinal forces in the cars automatic couplers as train electrodynamic braking. Procedia Engineer. 2016;134:415-421. https://doi.org/10.1016/j.proeng.2016.01.032
[43] Yan HB, Feng SS, Yang XH, Lu TJ. Role of cross-drilled holes in enhanced cooling of ventilated brake discs. Appl Therm Eng. 2015;91:318-333. https://doi.org/10.1016/j.applthermaleng.2015.08.042
[44] Yan HB, Zhang QC, Lu TJ. Heat transfer enhancement by X-type lattice in ventilated brake disc. Int J Therm Sci. 2016;107:39-55. https://doi.org/10.1016/j.ijthermalsci.2016.03.026
[45] Zaitong International Trading Co. Ltd. https://www.zhonganzt.com/pl/train-high-speed-rail-freight-car-brake-disc/ (accessed on 14.02.2024)